Ternary and Quaternary Uranium and Thorium Chalcogenides

Amy A. Narducci and James A. Ibers*

Department of Chemistry, Northwestern University, 2145 Sheridan Road, Evanston, Illinois 60208-3113

Received April 1, 1998. Revised Manuscript Received June 23, 1998

A survey of the structural chemistry of ternary and quaternary uranium (U) and thorium (Th) chalcogenides is presented. Specific attention is paid to the coordination environments of U and Th in a variety of classical and nonclassical structure types. The problems of defining the oxidation state of U from U—Q (Q = S, Se, Te) bond lengths and magnetic susceptibility data are also discussed.

Contents

Introduction

Interest in the chemistry of thorium (Th) and uranium (U) chalcogenides (chalcogen = Q = S, Se, Te) began in the late 1940s.[1] Early work centered mainly on the synthesis of solid-state binary chalcogenides; these were characterized almost entirely by X-ray powder diffraction techniques.[2−5] However, as better synthetic and analytical techniques became available, the focus of such research shifted to single-crystal studies of binary, ternary, and even quaternary systems. Though the structural chemistry of the actinides is often similar to that of some lighter transition metals, such as Zr and Hf, and to that of the lanthanides, the diffuse nature of the 5*f* orbitals leads to some differences and especially to interesting magnetic and electrical properties.

Despite the 50-year history of research in this area, the field remains remarkably narrow. Binary chalcogenide systems of both U and Th have been discussed in detail,[6−8] but only a few ternary systems have been studied in depth. Because most of the work on U and Th chalcogenides was completed before widespread use of single-crystal diffraction techniques, there are several systems for which little or no structural data are available. There is a paucity of information about Th chalcogenides because they have usually been assumed to be isostructural with related U compounds. The structural chemistry of the chalcogenides of the transuranium elements is far less developed. In this review we summarize some aspects of the structural chemistry of U and Th chalcogenides. We first consider the structures resulting from high-temperature, "brute-force" syntheses, and then discuss the structure types that have resulted from recent advances in synthetic methods, especially those from the reactive flux method.

Structure Types from Conventional Syntheses

ABQ_3. The best place to begin a discussion of the structure types of the U and Th chalcogenides is with the simplest structural motif. The familiar perovskite structure is the type adopted by ternary uranium sulfides and selenides of the formula ABQ_3. All of the ABQ_3 compounds form at high temperatures from stoichiometric reactions of the elements in their pure states, or more commonly from the binary chalcogenides. To grow single crystals, I_2 is typically used as a transport agent.[9,10] Uranium compounds of this stoichiometry are known for Sc,[11] V—Ni,[10,12−15] Pd,[16] Ru, Rh,[17] and Ba.[18,19] Thorium compounds are known for Cr, Fe, and Mn; however, no structural data are available for these Th compounds.[20] No telluride analogues have been reported. These compounds all possess the basic elements of the perovskite structure; namely, chains of corner-shared BQ_6 octahedra, with A cations in the interstitial sites. Typically, U or Th occupies the eight-coordinate A interstitial site with the smaller transition metal centering the BQ_6 octahedron. In $BaUS_3$, Ba occupies the A site and U the B site because Ba^{2+} has a larger ionic radius than U^{4+} (1.3 versus 0.89 Å).

There are two main subclasses of this structure type. Most of the ABQ_3 compounds crystallize in a three-dimensional structure (space group *Pnma*); however when B = Sc, Fe, or Mn, the compounds crystallize in a layered structure (space group *Cmcm*). The former structure (Figure 1) comprises chains of corner-shared BQ_6 octahedra; these chains are then linked together through corners of the octahedra to form a three-dimensional structure. In the normal perovskite ($CaTiO_3$) structure, the A cations (Ca) are coordinated to 12 anions at the corners of a cuboctahedron. However, in the related U and Th compounds, the environment of the A sites is distorted in such a way that A is

10.1021/cm9802200 CCC: $15.00
Published on Web 09/10/1998

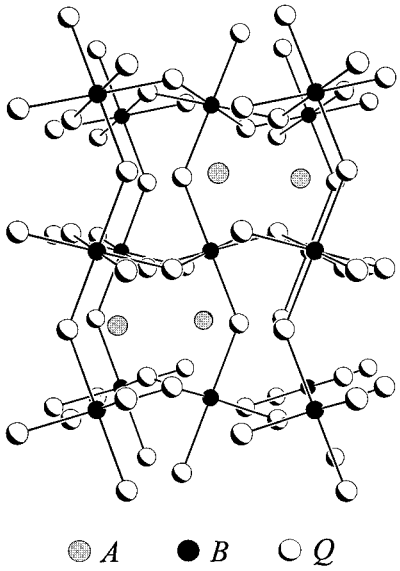

Figure 1. The ABQ_3 structure type in space group *Pnma*. Bonds to the *A* cations have been removed for clarity. Here and in all other figures, atoms are of arbitrary size.

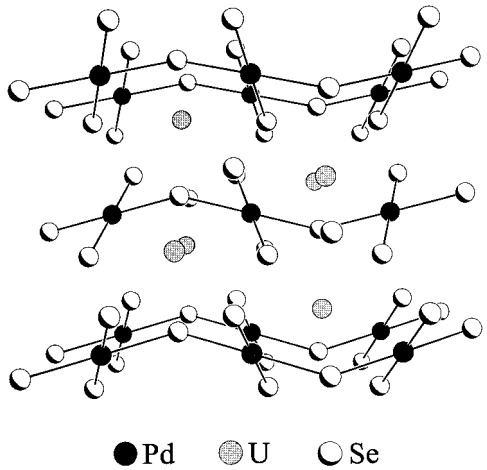

Figure 2. Structure of $PdUSe_3$ showing the square-planar environment of the Pd atoms. Bonds to U have been removed for clarity.

coordinated to eight anions at the corners of a bicapped trigonal prism. This distortion arises from tilting of the BQ_6 octahedra, which is necessary to accommodate the smaller size of the *A* cation. $PdUSe_3$ (Figure 2) offers an interesting exception to the usual perovskite structure. Because Pd prefers square-planar coordination, the *B* octahedral site is distorted in such a way that the two apical Se atoms are removed from the coordination sphere of Pd.

The reason for the formation of layered (*Cmcm*) structures for the Sc, Fe, and Mn compounds has never been adequately addressed. These compounds (Figure 3) form slabs of BQ_6 octahedra sharing corners in one direction and edges along the other. The U or Th atoms, still with the eight-coordinate bicapped trigonal-prismatic coordination environment, occupy the interlayer sites. Table 1 lists the unit cell parameters, the space group, and the calculated density for each of the ABQ_3 compounds of U studied by single-crystal X-ray diffraction techniques.[21−23] There are no obvious trends apparent in the data in Table 1.

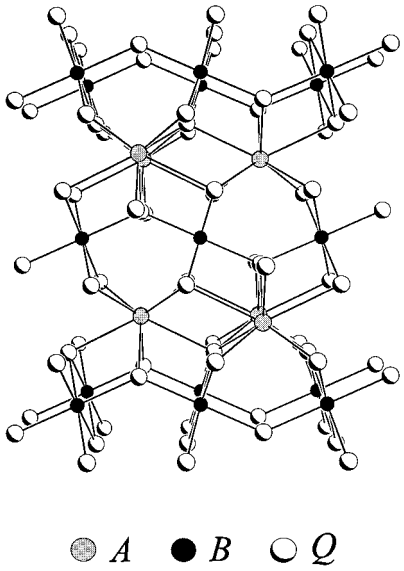

Figure 3. Layered ABQ_3 structure type in space group *Cmcm*.

Table 1. Unit Cell Constants, Space Groups, and Calculated Densities of ABQ_3 Compounds of U

B	*a*, Å	*b*, Å	*c*, Å	space group	density, g/cm^3	ref
			sulfides			
K	3.99	5.36	20.56	unknown	5.639	85
Sc	3.765(2)	12.134(6)	9.176(5)	*Cmcm*	6.008	11
V	6.974(2)	9.001(4)	6.124(2)	*Pnma*[a]	6.655	10
Cr	7.163(3)	8.851(3)	6.095(2)	*Pnma*[a]	6.639	10
Fe	3.795(3)	11.626(5)	8.717(4)	*Cmcm*	6.736	9, 15
Co	6.990(5)	8.625(8)	5.914(5)	*Pnma*[a]	7.324	9, 14
Ni	6.896(6)	8.793(8)	6.076(6)	*Pnma*[a]	7.084	9
Ru	6.939(2)	8.770(3)	5.896(2)	*Pnma*[a]	8.058	17
Rh	7.119(2)	8.618(2)	5.978(2)	*Pnma*[a]	7.916	17
Ba (*A*)	7.4823(5)	10.3801(7)	7.2148(5)	*Pnma*	5.590	18, 19
			selenides			
V	7.278(3)	9.405(4)	6.380(3)	*Pnma*[a]	7.998	12
Cr	7.484(4)	9.276(4)	6.382(2)	*Pnma*[a]	7.889	12
Mn	3.929(3)	12.771(5)	9.194(3)	*Cmcm*	7.629	12
Fe	3.942(3)	12.206(5)	9.117(4)	*Cmcm*	8.036	12
Co	7.338(5)	9.063(6)	6.229(4)	*Pnma*[a]	8.560	12
Ni	7.540(4)	8.976(5)	6.223(3)	*Pnma*[a]	8.416	12
Pd	8.130(3)	8.717(2)	6.271(2)	*Pnma*[a]	8.688	16

[a] Originally given in nonstandard setting.

AB_2Q_5. Most of the ABQ_3 compounds decompose into an AB_2Q_5 phase upon heating at temperatures >1200 °C. These AB_2Q_5 compounds can be synthesized in a rational manner by reactions of the binary metal chalcogenides at 800−1300 °C. Ternary compounds of the type AB_2Q_5 (B = U; Q = S, Se) are found for A = La−Gd,[24−26] Ca, Ba, Sr, Pb,[27−29] as well as Ti, Zr, Fe, Co, and Ni.[9,10,12,30] It has been postulated that, because of the ionic sizes involved, only the lighter lanthanides will form this structure type.[25] Most of these compounds are isostructural to the U_3Q_5 parent structure (vide infra). However the Fe, Co, and possibly Ni compounds form structures, shown in Figure 4, that are more closely related to those of the ABQ_3 compounds. $SrTh_2Se_5$[31] is the only ATh_2Q_5 compound to be characterized structurally, but the compounds $FeTh_2Q_5$ (Q = S, Se)[20] have been synthesized.

To understand fully the ternary AB_2Q_5 compounds we first must examine the structure of the binary parent compound, U_3Q_5. This structure[32] (Figure 5) possesses two crystallographically independent U sites, one mono-

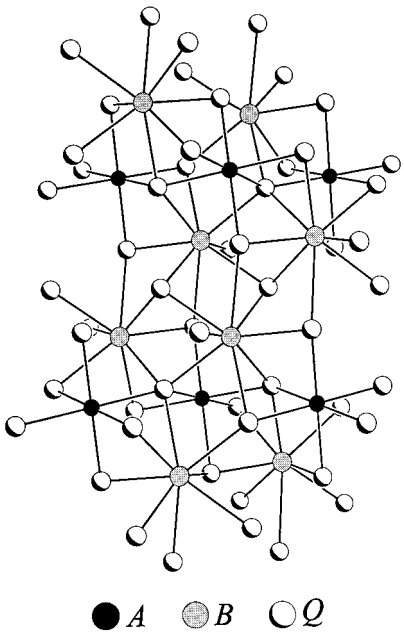

Figure 4. Structure of AB_2Q_5 for A = Fe, Co, and possibly Ni.

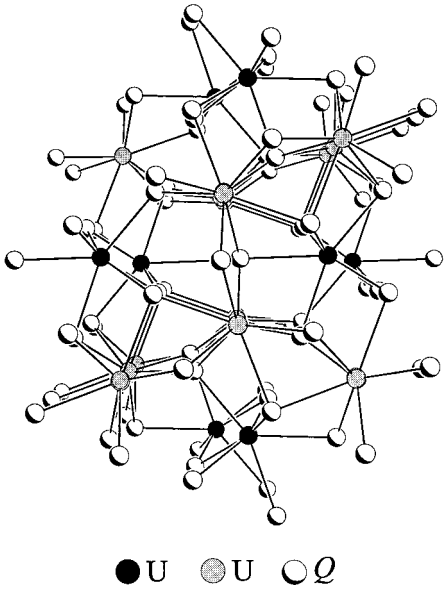

Figure 5. Structure of U_3Q_5. Light circles represent seven-coordinate U atoms. Dark circles represent eight-coordinate U atoms.

capped octahedral and one bicapped trigonal prismatic. The formal charges can be assigned as $U^{4+}(U^{3+})_2(Q^{2-})_5$, because there are no Se—Se bonds. The U^{3+} cations occupy the bicapped trigonal prismatic sites. Both divalent and trivalent metal ions can be substituted into the U_3Q_5 structure to form compounds of the formula $M_xU_{3-x}Q_5$. For the divalent cations the maximum value of x is 1, because as M^{2+} substitutes for U^{3+} another U^{3+} converts to U^{4+} (eq 1).

$$M^{2+} + U^{4+}(U^{3+})_2(Q^{2-})_5 \rightarrow M^{2+}(U^{4+})_2(Q^{2-})_5 \quad (1)$$

Such a substitution reduces the symmetry of the structure from orthorhombic to monoclinic (with β = 90°), with subsequent splitting of the bicapped trigonal prismatic site into two crystallographically distinct

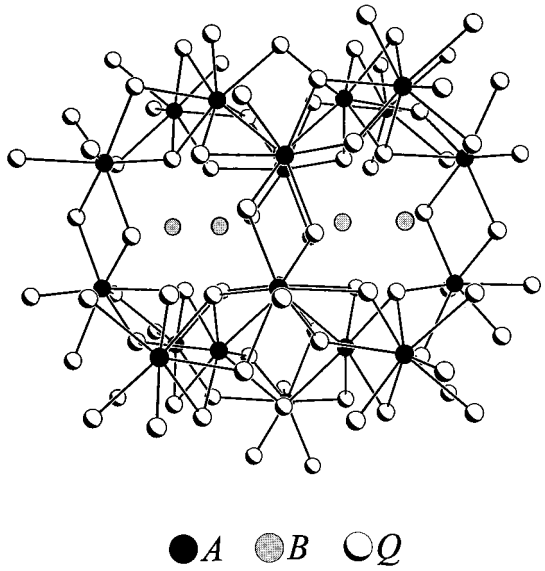

Figure 6. Structure of AB_2Q_5. Bonds to the A cations have been removed for clarity. The A cations sit in eight-coordinate bicapped trigonal-prismatic sites.

positions. The non-U metal atoms always substitute into one of the bicapped trigonal prismatic sites, perhaps because of their larger ionic radii, which are >1.00 Å in most cases (Figure 6). Of the structures that have been characterized by single-crystal X-ray diffraction techniques, all crystallize in the space group $P2_1/c$ with β = 90°. The same situation prevails in the only structurally characterized and related Th compound, $SrTh_2Se_5$.[31] For the trivalent cations, the maximum value of x is 2, corresponding to the formula M_2UQ_5, and to substitution of the U^{3+} site ($(M^{3+})_2U^{4+}(Q^{2-})_5$). In this instance the structure remains orthorhombic and isostructural with U_3Q_5. There have been several Th analogues reported for the type Ln_2ThS_5,[25] where Ln = La—Sm and U, as well as several quaternary compounds $LnThUS_5$, where Ln = La—Sm.[25]

***MU*$_8$*Q*$_{17}$.** Compounds of the type MU_8Q_{17} were discovered and reported along with the ABQ_3 and AB_2Q_5 compounds, and so we discuss them here. These compounds are formed at ~1000—1200 °C from either stoichiometric reactions of the elements or from combinations of the binary metal chalcogenides. They are known for Q = S, Se and M = Mg, Sc—Ni,[9,10,12,33–35] and Lu.[35] No related Th compounds are known.

The MU_8Q_{17} compounds crystallize in the structure shown in Figure 7. The U atoms are located in three crystallographically distinct sites: one bicapped trigonal-prismatic and the other two highly deformed dodecahedral. MQ_6 octahedra sit at the corners of the unit cell and at the center of the C-face. They are isolated from each other by the various U polyhedra. Thus, the MQ_6 octahedra share no Q atoms with each other. The structure is built up from chains of the U polyhedra. The bicapped trigonal prisms share edges and caps to form infinite chains (P). The two distinct dodecahedra form edge-shared chains (D, D′). These chains alternate P—D—P—D′—P—, and M atoms fill the octahedral holes formed by the chains.

***AnYQ*.** Compounds of the $AnYQ$ type are found for almost all permutations of An = U, Th; Y = O, N—Bi, Si—Sn; and Q = S, Se, Te. Table 2 is a listing of the

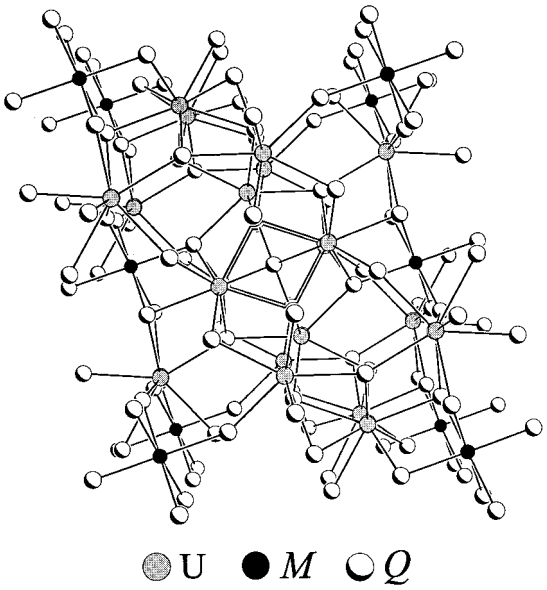

Figure 7. Structure of MU_8Q_{17}.

Table 2. Structure Types of Known *AnYQ* Compounds

Th*YQ*	structure type	ref	U*YQ*	structure type	ref
ThOS[a]	PbFCl	44	UOS[a]	PbFCl	44
ThOSe[a]	PbFCl	2	UOSe[b]	PbFCl	43
ThOTe[b]	PbFCl	4, 40	UOTe[c]	PbFCl	41
ThSiS[a]	anti-Ti_2Bi	36	USiS[c]	PbFCl	37
ThSiSe[a]	anti-Ti_2Bi	36	USiSe[a]	PbFCl	37
ThSiTe[a]	anti-Ti_2Bi	36	UGeS[c]	PbFCl	37
ThGeS[b]	anti-Ti_2Bi	36	UGeSe[c]	anti-Ti_2Bi	37
ThGeSe[a]	anti-Ti_2Bi	36	UGeTe[c]	anti-Ti_2Bi	37
ThGeTe[a]	anti-Ti_2Bi	36	USnTe[c]	PbFCl	37
ThNSe[a]	PbFCl	47	UNSe[a]	PbFCl	47
ThNTe[a]	PbFCl	47	UNTe[c]	PbFCl	47
ThPS[a]	PbFCl	45	UPS[b]	PbFCl	46
ThPSe[a]	PbFCl	45	UPSe[b]	PbFCl	45
ThAsS[a]	PbFCl	45	UPTe[c]	anti-Ti_2Bi	39
ThAsSe[b]	PbFCl	45	UAsS[b]	PbFCl	38, 45
ThAsTe[b]	PbFCl	45	UAsSe[b]	PbFCl	38, 45
ThSbSe[a]	PbFCl	45	UAsTe[b]	anti-Ti_2Bi	38, 39
ThSbTe[a]	PbFCl	45	USbS[a]	PbFCl	37, 45
ThBiTe[a]	PbFCl	45	USbSe[b]	PbFCl	37, 45
			USbTe[b]	PbFCl	37, 45
			UBiTe[a]	PbFCl	

[a] Unit cell from powder data only. [b] Single-crystal structure data. [c] Structure from powder data only.

known compounds of this type. These compounds form from stoichiometric reactions of the elements at temperatures between 700 and 1050 °C. There are two distinct subtypes of this group, both of which are related to the PbFCl structure type. Both subtypes include nine-coordinate *An* atoms in a capped square-antiprismatic environment. Four *Y* atoms form the "bottom" square face, whereas 4 + 1 *Q* atoms make up the top face and cap. The prisms share edges and corners to form layers that stack with an atom sequence *Y*−*An*−*Q*−*Q*−*An*−*Y*−. The two subgroups adopt either the anti-Ti_2Bi structure type (UGeTe)[36−39] or the PbFCl structure type.[2,4,37,38,40−47] The difference between the two structures lies in the way the antiprisms are connected. For the former, the antiprisms stack directly on top of one another, sharing 4*Y* faces (Figure 8a). For the latter, the true PbFCl structure (Figure 8b), the slabs formed by these antiprisms are off-set so that they share *edges* of the 4*Y* faces. Which structure type a

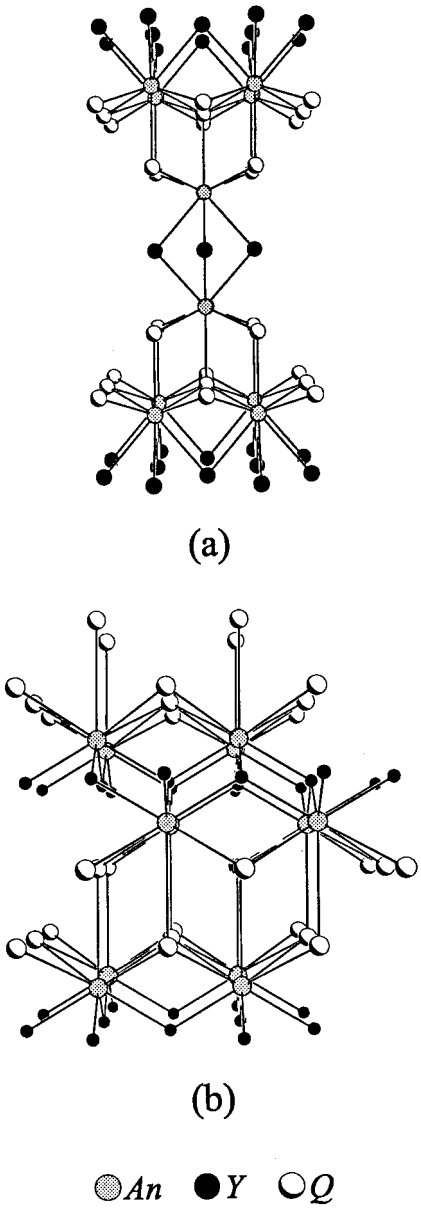

Figure 8. Comparison of the structures *AnYQ*: (a) anti-Ti_2Bi structure type and (b) PbFCl structure type.

given compound will possess is dependent on the radius ratio r_Y:r_Q and the size of *An*. If r_Y:r_Q is small and *An* is large, the compound will adopt the anti-Ti_2Bi structure type. If the situation is reversed, *An* is small and r_Y:r_Q is large, the compound will adopt the PbFCl structure type.

***An*$_2$N$_2$*Q*.** Compounds of the type An_2N_2Q, where *An* = U, Th and *Q* = S, Se, Te, form from reactions of the binary chalcogenides at 1000−1200 °C. These compounds possess elegant structures that are closely related to the *AnYQ* family. There are two subgroups of the An_2N_2Q type, again as a function of ionic size.[48,49] When *Q* = S, Se the compounds adopt the Ce_2O_2S structure type shown in Figure 9a. The *An* atoms have a capped triangular antiprismatic environment. Three *Q* atoms comprise one face of the prism, whereas four N atoms make up the opposite face and cap. The antiprisms share corners in one dimension and edges along the other to form slabs that stack by sharing corners and caps of the common faces. The Ce_2O_2S

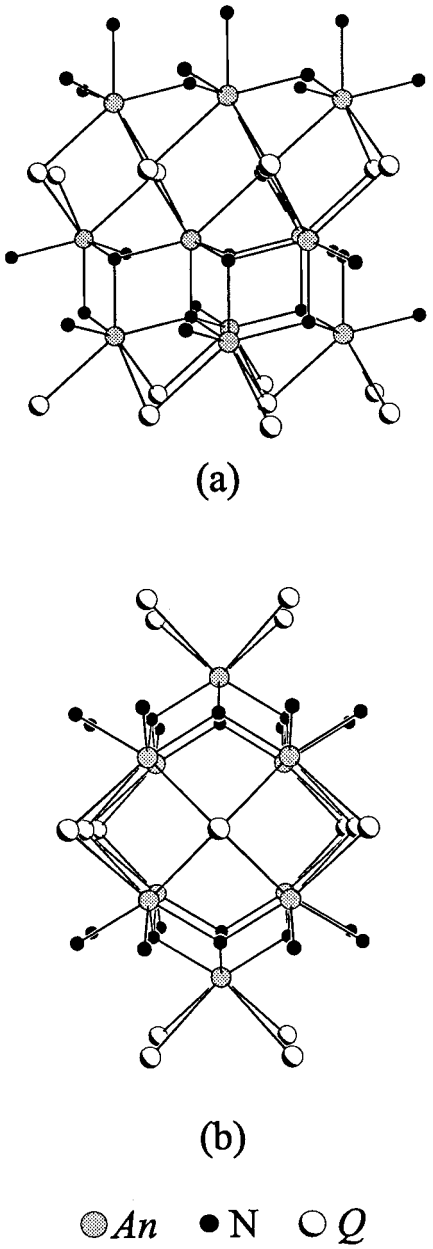

Figure 9. Comparison of the structures An_2N_2Q: (a) Q = S, Se and (b) Q = Te.

structure type cannot accommodate Te with its larger ionic radius. Thus, the compounds An_2N_2Te adopt a body-centered tetragonal structure, shown in Figure 9b. Once again, *An* atoms are sandwiched between N and Te layers and are found in distorted square-antiprismatic sites. In this subgroup, these antiprisms lack additional capping *Q* atoms and the *An* atom is only eight-coordinate. As expected, the *An* atoms also sit much closer to the N atoms than to the *Q* atoms and therefore the prisms are highly distorted. Compounds of these types are also found for the pnictides,[48,49] with P and As forming the Ce_2O_2S structure and Sb and Bi forming the An_2N_2Te structure. The compound U_2O_2Te[50] is the only known example of an oxide of this group with this latter structure.

Oxychalcogenide Compounds. Although there is a plethora of oxychalcogenide compounds, we consider here only those with formal *An*—*Q* bonds. We thus ignore a number of uranyl chalcogenides in which the U atoms are coordinated only to O atoms in various polyhedra.

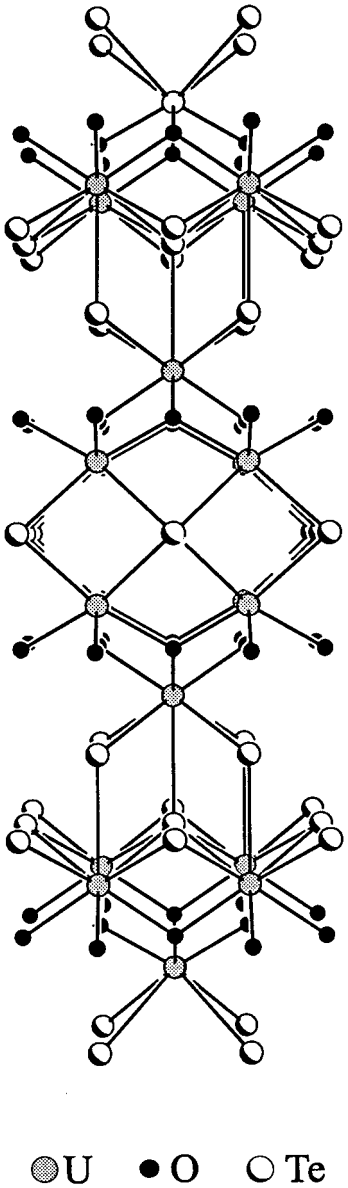

Figure 10. Structure of $U_4O_4Te_3$. Note the UOTe and U_2O_2-Te layers as compared with Figures 8b and 9b.

The compound $U_4O_4Te_3$,[51] the only known actinide-oxychalcogenide with this stoichiometry, forms a structure that combines the basic building blocks of the *AnYQ* and An_2N_2Q structures. Body-centered slabs of U_2O_2Te reminiscent of the An_2N_2Te compounds are sandwiched between PbFCl-type slabs of UOTe, as shown in Figure 10.

The reaction of UOS with a variety of binary rare-earth sulfides at temperatures from 1400 to 1900 °C leads to the compounds $(UOS)_nLnS$, where for n = 2, *Ln* = Gd—Lu, Y,[52] and for n = 4, *Ln* = Lu.[53] These structures comprise PbFCl-type slabs of UOS separated by a two-dimensional layer of corner-shared LnQ_6 octahedra. For n = 2, the LnQ_6 octahedra separate single UOS slabs, as shown in Figure 11. For n = 4, the UOS slabs are doubled, as in Figure 12.

***An*P_2S_6.** The thiophosphate compounds AnP_2S_6 are known for *An* = U, Th.[54,55] These form from reactions of the elements at 750−800 °C. Here the structure

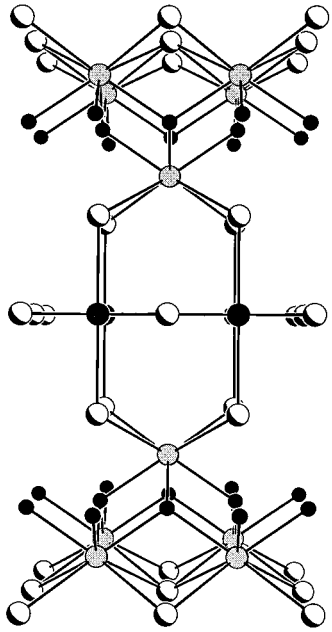

Figure 11. Structure of $(UOS)_2LnS$. Note the single PbFCl-type layers (see Figure 8b).

comprises a network of AnS_8 dodecahedra linked by P_2S_6 units to form a two-dimensional channel network (Figure 13). The AnS_8 dodecahedra result from the placement of *An* atoms at the centers of tetrahedra formed by four PS_2 units.

***An*Mo$_6$*Q*$_8$.** These compounds (*An* = U, Th)[56] are synthesized by stoichiometric reactions of AnQ_2, MoQ_2, and Mo powder at ~1300 °C. They crystallize with the typical Chevrel-phase structure,[57] with Mo_6 octahedra capped by eight *Q* atoms on each face and *An* atoms coordinated by eight *Q* atoms in the cubic vacancies (Figure 14).

Valence electron counts for typical Chevrel-phase compounds show that the Mo_6 core has 20 e^-. Subsequent filling of the vacancies by metal atoms leads to charge transfer from the metal to the Mo_6 core, up to a total of 24 e^-. No compounds of this type are known that have a total count of exactly 24 e^-. The U^{4+} and Th^{4+} ions should supply exactly 4 e^- per cluster. However, UMo_6Se_8 and $ThMo_6S_8$ are nonstoichiometric, with an *An* occupancy of ~82%, and the U atoms in UMo_6S_8 are said to have an nonintegral oxidation state.

Cu$_2$U$_3$*Q*$_7$ and Cu$_2$U$_6$*Q*$_{13}$. $Cu_2U_3Q_7$[58] and $Cu_2U_6Q_{13}$[59,60] (*Q* = S, Se) form from reactions of the metal chalcogenide binaries at lower temperatures, 600 and 800 °C, respectively. The structure of $Cu_2U_3Q_7$ (Figure 15) contains trigonal planar CuQ_3 units that stack along the corners of the unit cell. Double chains of UQ_8 polyhedra run through the middle of the unit cell, with CuQ_4 squashed tetrahedra filling in the holes between UQ_8 units. The compound $Cu_2U_6Q_{13}$ (Figure 16) comprises layers of trigonal prismatic CuQ_3 units and dodecahedral UQ_8 polyhedra; the layers alternate Cu−U−U−Cu. Given that these structures possess no *Q*−*Q* bonds and that Cu is almost invariably Cu^{1+} in chalcogenide compounds, the assignment of U^{4+} follows.

UPd$_3$S$_4$, U$_2$PdS$_4$, and UPd$_2$S$_4$. These compounds form from stoichiometric reactions of US_2 with elemental Pd and S at 900 °C. UPd_3S_4,[61] shown in Figure 17, has the platinum-bronze structure type. This structure comprises cubic US_8 units stacked along the corners of the unit cell, stitched together through square-planar PdS_4 units. The structure of U_2PdS_4[62] (Figure 18a) contains seven-coordinate U atoms in irregular polyhedra. The U atoms are coordinated to three S atoms of a triangular face and four additional S atoms of the opposite square face (Figure 18b). The Pd atoms occupy the centers of highly distorted S_4 tetrahedra (Figure 18c) formed from the S atoms of the triangular faces of the US_7 units. The compound UPd_2S_4[63] (Figure 19) contains square-planar PdS_4 units and US_8 polyhedra that can best be described as deformed square antiprisms.

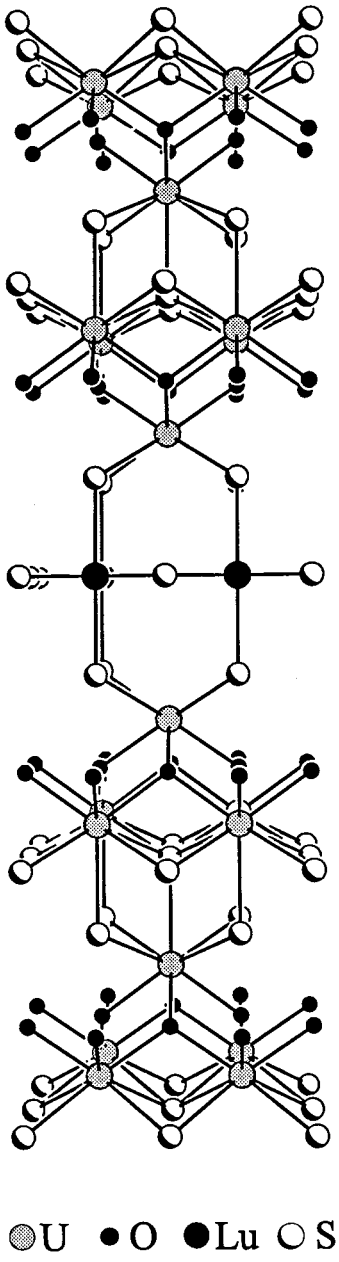

Figure 12. Structure of $(UOS)_4LuS$. Note the double PbFCl-type layers as compared with Figures 8b and 11.

ScU$_3$S$_6$. In addition to the $ScUS_3$ and ScU_8Q_{17} types discussed previously, the compound ScU_3S_6 is known.[64] It forms from the reaction of UO_2 with Sc_2O_3 in a stream of H_2S at 1350 °C. The structure of ScU_3S_6[64] is shown in Figure 20. Though overall it bears a close resem-

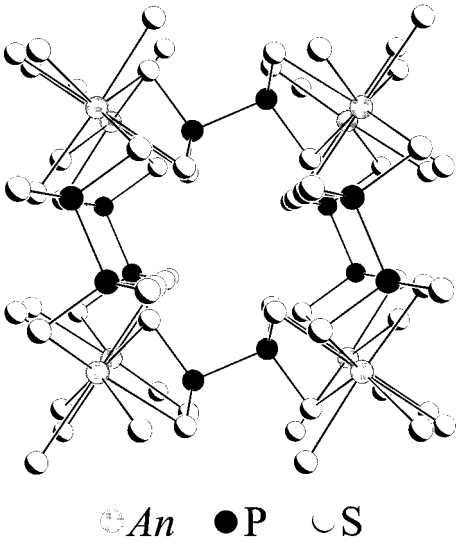

Figure 13. Structure of AnP_2S_6.

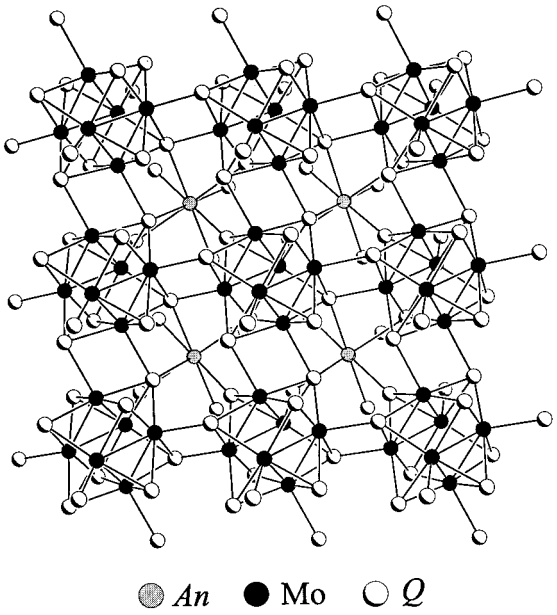

Figure 14. Structure of $AnMo_6Q_8$.

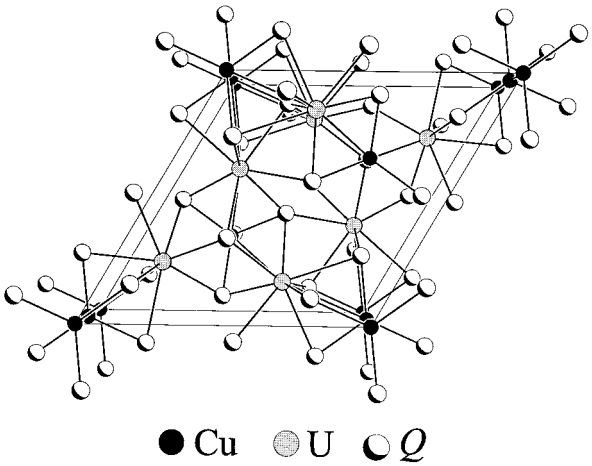

Figure 15. Structure of $Cu_2U_3Q_7$ showing the staggered CuQ_3 units along the unit cell edges.

blance to the *Cmcm* ABQ_3 compounds, the U coordination environments are closer to those found in the AB_2Q_5 structure. There are three crystallographically unique U atoms in ScU_3S_6; two are in bicapped trigonal-prismatic sites and the third is in a seven-coordinate capped octahedral site. ScS_6 octahedra are linked through edges to form infinite, though isolated, chains.

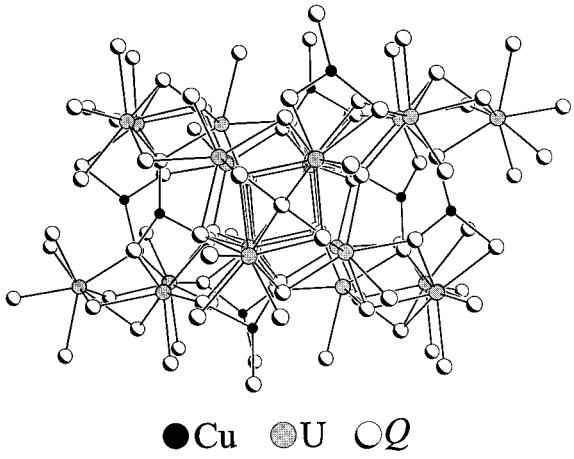

Figure 16. Structure of $Cu_2U_6Q_{13}$.

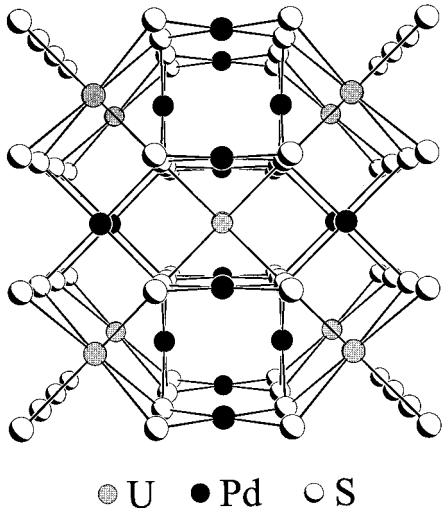

Figure 17. Structure of UPd_3S_4 showing the cubic US_8 units and the PdS_4 square-planar units.

***M*$_2$U$_6$*Q*$_{15.5}$.** Compounds of the type $M_2U_6Q_{15.5}$ (M = Rh, Ir; Q = S, Se)[65] form from reactions of UQ_2 with M and Q at temperatures around 1100 °C. $Rh_2U_6S_{15.5}$ forms in the reaction of US_2 with Rh and S in a stream of H_2S at 1400 °C. These compounds crystallize with a three-dimensional channel structure built up of MQ_6 octahedra surrounded by UQ_8 bicapped trigonal prisms (Figure 21). One independent Q atom occupies the channels and is weakly coordinated to 12 other Q atoms at distances >3.0 Å (Q = Se).

Structure Types from Reactive Flux Syntheses

With the discovery of low-temperature synthetic techniques, especially the reactive-flux method,[66] a variety of lower-dimensional structures have been synthesized and characterized. The reactive-flux method has been applied to U and Th chalcogenide chemistry[67] and has resulted in a series of channel, layered, and even infinite chain structures that differ markedly from the classic structures discussed earlier.

***AAn*$_2$*Q*$_6$.** Whereas U, rather than Th, dominates the compounds already described, the only U compound of

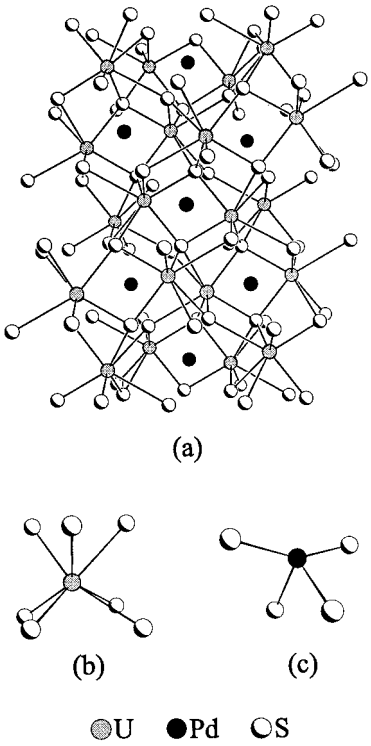

Figure 18. Views of (a) the structure of U_2PdS_4 with bonds to Pd atoms removed for clarity; (b) US_7 polyhedron; and (c) PdS_4 squashed tetrahedron.

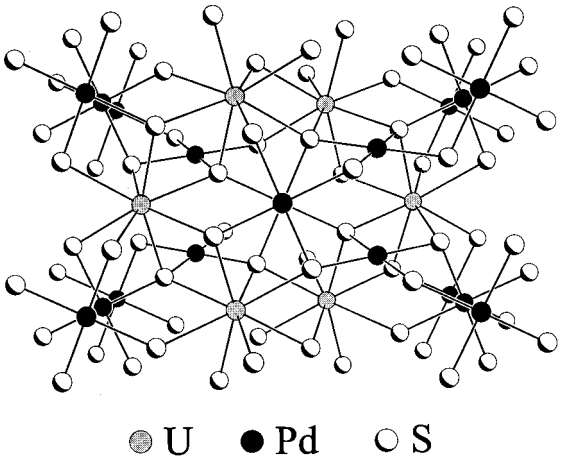

Figure 19. View of UPd_2S_4 showing the staggered, square-planar PdS_4 units through the center of the unit cell and along the edges.

this type is $Tl_{0.56}UTe_3$,[68] the rest being ATh_2Q_6 where A = K, Cs, Cu, and Q = Se, Te.[31,69,70] Compounds of the type ATh_2Q_6, where A = K, Cs, form with the aid of an A_2Q_3 flux at 600−650 °C; the Tl analogue forms at 600 °C from a reaction of the elements; and the Cu compound crystallizes without the aid of a flux from a reaction of the elements at 1000 °C.

The AAn_2Q_6 structure is closely related to the UTe_2[71] and $ZrSe_3$[72,73] structure types. In these two binaries, metal atoms are again coordinated by eight Q atoms in a bicapped trigonal prism. These prisms link together by sharing vertices and capping Q atoms to form infinite chains. In UTe_2, these chains form a three-dimensional network by sharing the uncapped faces of the MQ_8 prisms, as shown in Figure 22a. In $ZrSe_3$, the layers are separated by a van der Waals gap (Figure 22b). In

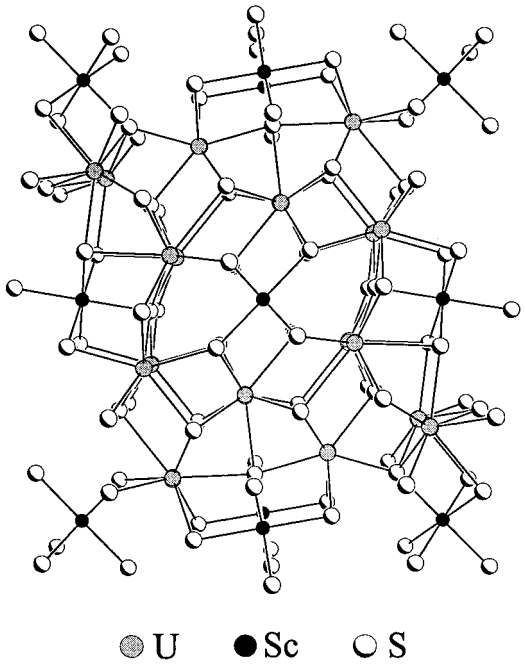

Figure 20. Structure of ScU_3S_6.

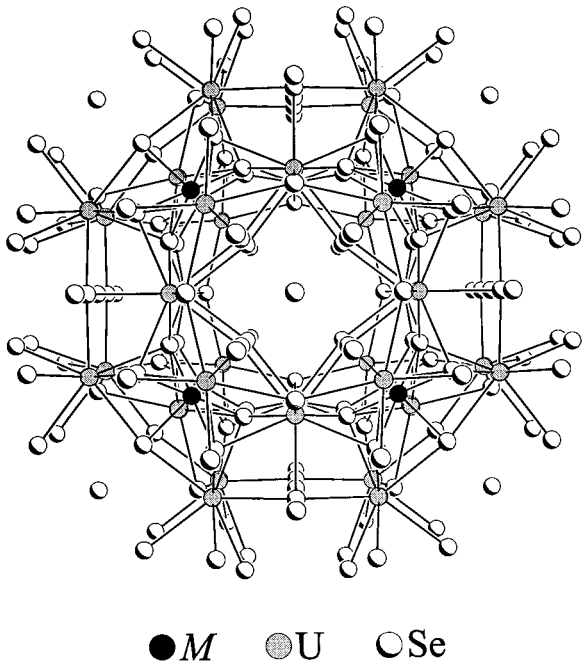

Figure 21. View of $M_2U_6Q_{15.5}$ showing the isolated Se atoms in the centers of the channels.

the AAn_2Q_6 structure, these A cations force the layers apart by weakly coordinating to the eight Q atoms of the uncapped faces (Figure 23a). Only the Cu analogue remains a three-dimensional structure with the Cu atoms formally bound tetrahedrally to four Te atoms, two from each uncapped face (Figure 23b).

The infinite chain in the AAn_2Te_6 structure gives rise to short Te−Te contacts ranging from 3.05 to 3.11 Å that fall between the single bond distance (2.76 Å) and van der Waals separation of Te^{2-} anions (4.10 Å) and hence to a nonintegral oxidation state for each Te−Te unit. Thus we would expect high electrical conductivity along these infinite Te−Te chains, but rather weak conductivity in directions perpendicular to the chains. Because of the crystal morphology, only measurements orthogo-

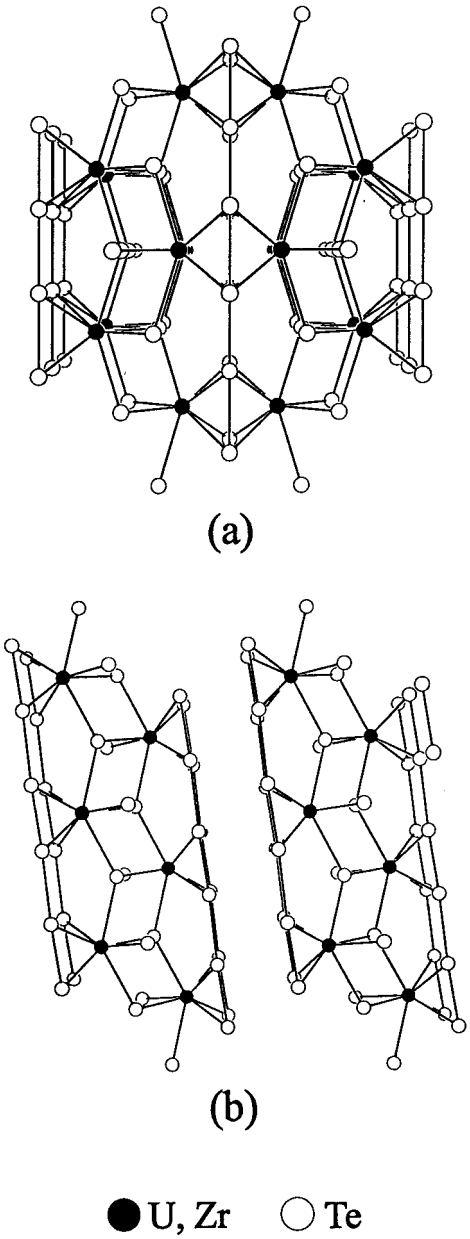

Figure 22. Comparison of the structures of (a) UTe_2 and (b) $ZrTe_3$.

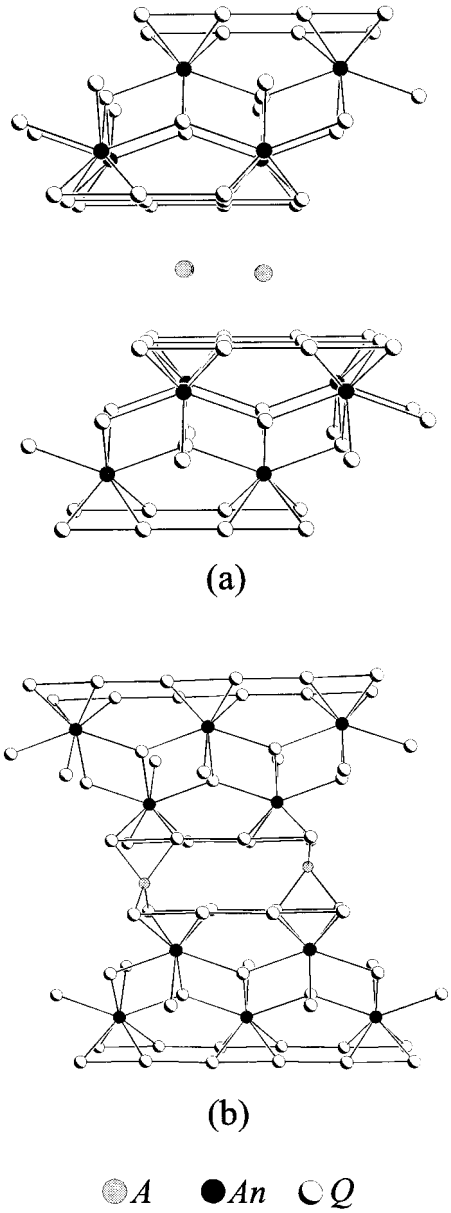

Figure 23. Comparison of the structures of the AAn_2Q_6 compounds: (a) A = K, Cs, Tl; and (b) A = Cu.

nal to the Te−Te chains have been made and semiconducting behavior is found.

$CsUTe_6$. The compound $CsUTe_6$[67,74] (Figure 24) was formed in an attempt to synthesize a quaternary Cs/Ag/U/Te compound by reacting elemental Ag, U, and Te with a Cs_2Te_3 flux first at 650 °C and then at 900 °C. $CsUTe_6$ has a one-dimensional structure unique to the ternary uranium chalcogenides. The U atoms are coordinated to nine Te atoms in a tricapped trigonal prismatic environment. These UTe_9 prisms share triangular faces to form infinite chains. Two capping Te atoms from neighboring chains are bound by a distance of 2.795(9) Å to link two chains together. The Cs atoms are situated between the $^1_\infty[U_2Te_{12}^{2-}]$ chains, coordinated to nine Te atoms. Several lanthanide compounds have been reported with this same stoichiometry.[75−78] However, their structures are not known.

Quaternary Compounds. Compounds of the type $AMRQ_3$, where A = alkali or alkaline earth metal, M = 3d metal; R = rare-earth element, Zr, or Hg; and Q = S, Se, Te, have been known for some time.[79−82] Recently this system has been expanded to include U and Th in place of R.[74,83,84] These compounds form with the aid of an A_2Q_x flux at 400 °C and crystallize with a two-dimensional layered structure with the A cations in the interlayer spacing. The layers are formed by edge- and corner-shared RQ_6 (or AnQ_6) octahedra, with the M elements filling the tetrahedral sites (Figure 25). These compounds can be related to the $FeUS_3$-type[15] discussed earlier (Figure 3). If we insert M atoms into the tetrahedral sites of the $FeUS_3$ structure and substitute R for Fe and A for U, we arrive at the $AMRQ_3$ family of compounds. Once again, the R atom occupies the octahedral site and the larger A atom occupies the eight-coordinate bicapped trigonal-prismatic site.

A very different layered structure is found in the compound $CsTiUTe_5$,[74] which was synthesized by a reactive flux technique at 600 °C and then 900 °C. The layers are formed by single chains of face-shared $TiTe_6$

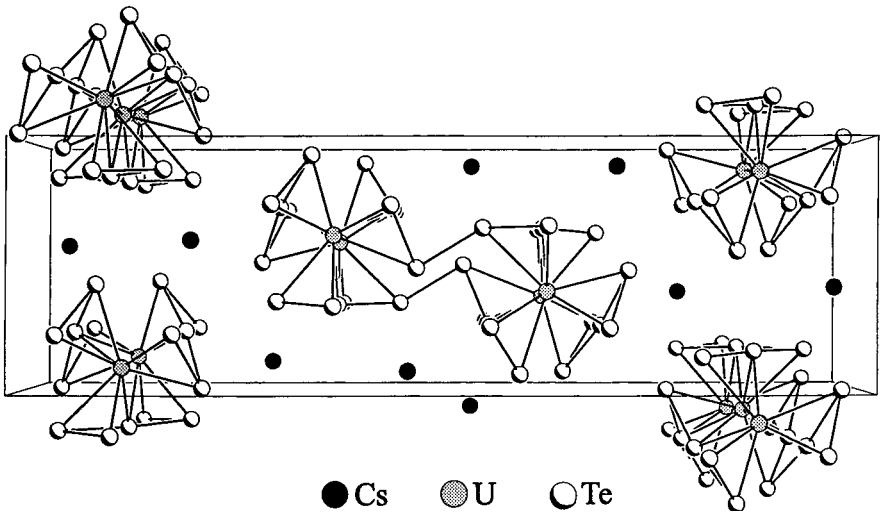

Figure 24. View of $CsUTe_6$ looking down the U_2Te_{12} double chains.

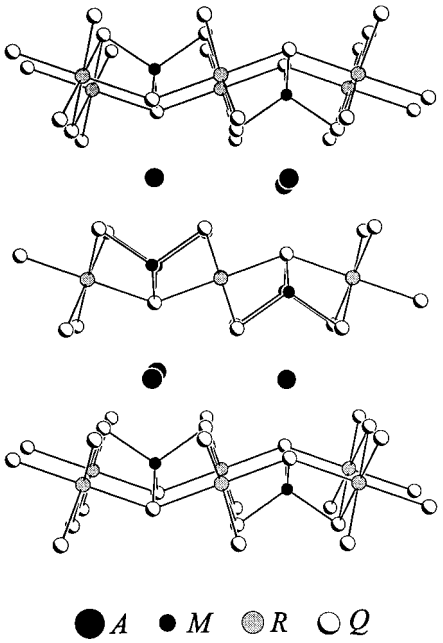

Figure 25. Structure of $AMRQ_3$.

octahedra connected by double chains of edge-shared UTe_8 bicapped trigonal prisms (Figure 26). The Cs atoms sit between the layers, coordinated to 10 Te atoms at the corners of a pentagonal prism. The Te atoms that form the shared edges of the UTe_8 bicapped trigonal prisms are separated by only 3.065(1) Å, which is similar to the Te−Te interactions of the AAn_2Te_6 compounds. Single-crystal resistivity measurements along the infinite Te−Te chains indicate semiconducting behavior, though one would expect the conductivity to be high along the chains. Again we see the problems of formal charge assignment in a structure with intermediate Te−Te contacts. For $CsTiUTe_3$, however, magnetic susceptibility measurements lead to an effective magnetic moment (μ_{eff}) of 2.23(1) μ_B, which is alleged to be indicative of U in an oxidation state between U^{4+} and U^{5+}.[74,85]

The compound $Cs_8Hf_5UTe_{30.6}$ forms from a reaction of the elements with a Cs_2Te_3 flux at 700 °C. If we ignore the nonstoichiometry, then $Cs_8Hf_5UTe_{30.6}$[67,74] forms a one-dimensional structure (Figure 27) of the $Cs_4Zr_3Te_{16}$ type.[86] The Hf and U atoms possess coordination numbers 7−9, and are found in capped trigonal-prismatic environments. There is no disorder between the Hf and U sites, and only one of the two chains contains U atoms. However, there is some disorder in the Te sites because of the Te deficiency. This structure includes seven Te−Te single bonds (2.705(8)−2.789(4) Å) and 16 Te−Te distances <3.07 Å. Because of these short distances, no attempt was made to assign formal oxidation states.

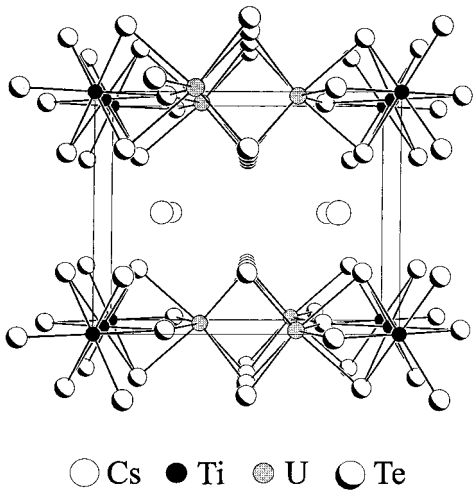

Figure 26. View of $CsTiUTe_5$ highlighting the layered aspect of the structure.

Two uranium selenophosphates, $K_2UP_3Se_9$[87] and $Rb_4U_4P_4Se_{26}$,[88] have been synthesized through the use of an A_2Se/P_2Se_5 (A = K, Rb) reactive flux at 490 and 500 °C, respectively. In both compounds, U is coordinated by nine Se atoms in a tricapped trigonal-prismatic environment. The USe_9 polyhedra of $K_2UP_3Se_9$ are stitched together by the selenophosphate units, $[P_2Se_6^{4-}]$ to form layers, with the K atoms separating the layers (Figure 28). A formal charge representation of the compound can be given by $K_4^{+}U_2^{4+}[P_2Se_6^{4-}]_3$. The structure of $Rb_4U_4P_4Se_{26}$ comprises a three-dimensional array of USe_9 tricapped trigonal prisms. These prisms are linked through Se^{2-} and Se_2^{2-} ligands to form infinite chains that are joined by $[PSe_4^{3-}]$ units to form a three-dimensional network structure with Rb atoms

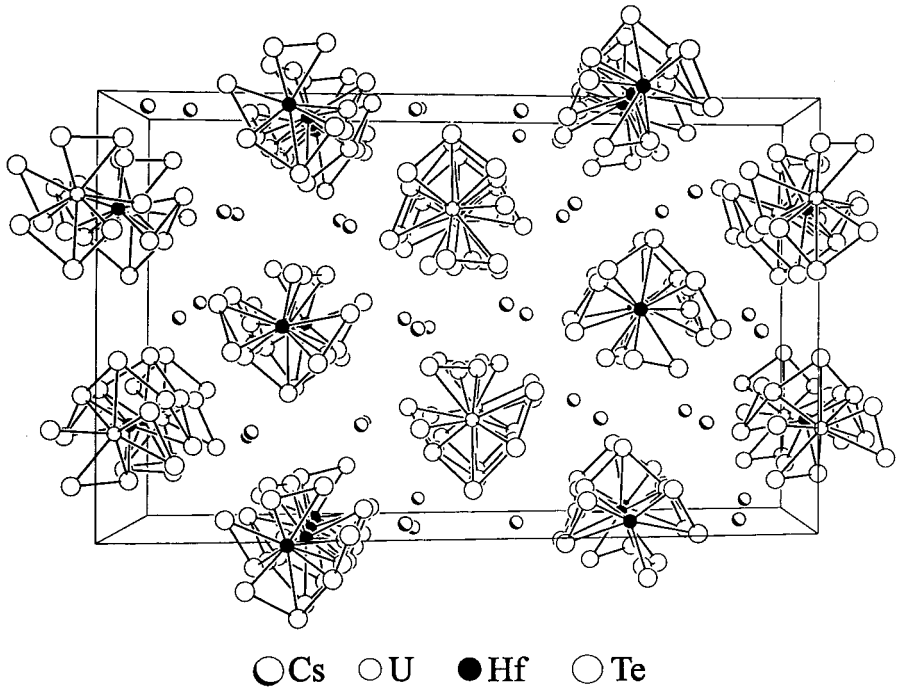

Figure 27. View of $Cs_8Hf_5UTe_{30.6}$ looking down the Hf−Te−U chains.

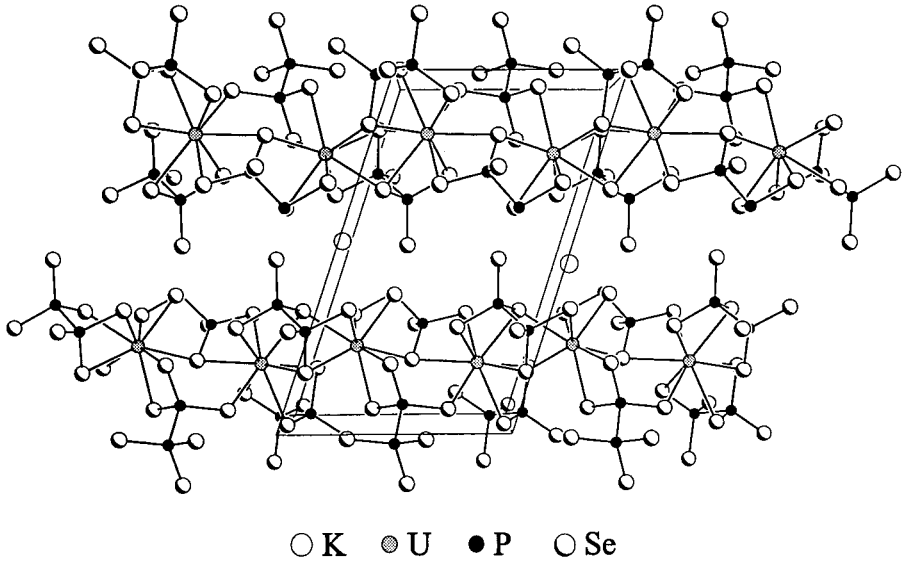

Figure 28. View of $K_2UP_3Se_9$ perpendicular to the $U_2[P_2Se_6]_3$ layers.

situated in the channels. The U atoms are bound to three Se_2^{2-} units, two $[PSe_4^{3-}]$ ligands through two Se atoms each, and one single Se^{2-} unit. The compound has been described formally as $Rb_4^{+}U_4^{5+}[PSe_4^{3-}]_4(Se^{2-})_2(Se_2^{2-})_4$. The formal oxidation state U^{5+} is unusual. KUS_3[85] provides another example of U^{5+}, although the compound has not been fully characterized by single-crystal X-ray diffraction techniques.

Discussion

From the descriptions presented in this review, it is obvious that U and Th, with large ionic radii, possess high coordination numbers in their chalcogenide structures. These numbers are no smaller than 6 and are usually 7−9, with 8 as a bicapped trigonal prism of chalcogen atoms being the most common environment. VSEPR theory[89] predicts little difference in energy among the variety of possible eight-coordinate environments, but dodecahedral and bicapped trigonal prismatic are somewhat more favorable.[90]

The propensity of the chalcogens, especially Te,[91] to form *Q*−*Q* bonds of lengths intermediate between the single bond and the van der Waals interaction often makes it impossible to assign formal oxidation states to U and Th in their chalcogenides. If *Q*−*Q* bond lengths cannot be used to assign formal oxidation states, are there other approaches? Effective magnetic moments and U−*Q* (or less often Th−*Q*) bond lengths have been used. As we shall illustrate, their use is fraught with peril.

Magnetic susceptibility measurements are often used to determine the oxidation state of U in the chalcogenides. In the Russell−Saunders coupling scheme the values for the effective magnetic moment are 3.58 μ_B

Table 3. Oxidation State and Mean U−S Bond Lengths for Eight-Coordinate Uranium

compound[a]	oxidation state	coordination number	⟨U−S⟩	ref
ScU_3S_6	3	8	2.874(5)	64
$ScUS_3$	3	8	2.924	11
ScU_3S_6	3	8	2.934(5)	64
CrU_8S_{17}	4	8	2.78	33
FeU_8S_{17}	4	8	2.781(3)	34
$RhUS_3$	4	8	2.810(3)	17
$Cu_2U_6S_{13}$	4	8	2.820(5)	59
CrU_8S_{17}	4	8	2.83	33
$Cu_2U_6S_{13}$	4	8	2.830(5)	59
FeU_2S_5	4	8	2.83	30
UPd_2S_4	4	8	2.830(3)	63
FeU_8S_{17}	4	8	2.833(3)	34
CrU_8S_{17}	4	8	2.84	33
$FeUS_3$	4	8	2.84	9
FeU_8S_{17}	4	8	2.846(3)	34
$CrUS_3$	4	8	2.85	10

[a] Compounds listed more than once represent bond lengths to multiple, distinct U atoms.

and 3.62 μ_B for U^{4+} and U^{3+}, respectively.[25] However, crystal field effects have a dramatic influence on values of μ_{eff} for U; values in the range 2.83−3.58 μ_B have been assigned to U^{4+} [60] and values as low as 3.34 μ_B to U^{3+}.[25]

From extensive data mainly on oxide structures, where ambiguities in formal oxidation state are minimal and where the hard-sphere concept of ionic radius is of some validity, tabulations of ionic radii as a function of formal oxidation state and coordination number have been derived.[92] In principle, *An*−*Q* bond lengths are also sensitive to the formal oxidation state and coordination number of *An*. However, meaningful trends are very difficult to discern. One problem is that the expected differences in ionic radii, say between U^{3+} and U^{4+}, for a given coordination number are often small compared with the variations in U−*Q* distances in a given structure. Thus, one is forced to take an average U−*Q* distance in that structure. Another problem is that when there are significant Q−Q interactions, the coordination polyhedra are often markedly distorted and the concept of coordination number is clouded. Finally, there is the "Catch-22" problem: to develop and use a correlation between bond length and oxidation state of *An*, one must "know" the oxidation state of *An* in a reasonable number of structures. An overview[93] of U−*Q* bond lengths as a function of the oxidation state of U has been given for a limited number of compounds. Though those and later data show some broad trends, our view of the structural results leads us to believe that a correlation of *An*−*Q* bond lengths with the oxidation state of *An* can only be made for coordination number 8 and *Q* = S. Here there are sufficient data, variations of *An*−S bond lengths are less severe, and S−S interactions are uncommon. Table 3 shows such a correlation, which is in line with the expectation that ionic radius decreases with increasing oxidation state. Data for coordination numbers other than 8 and for *Q* = Se or Te simply do not provide a sufficiently robust correlation to be useful in the assignment of formal oxidation states.

Conclusions

The structural chemistry of ternary and quaternary U and Th chalcogenides, though still a developing field of research, comprises a series of compounds extending from the classical perovskite type to elegant open-framework structures. Though many of the same building blocks are found throughout the range of compounds, many of the differences in U and Th chalcogenides are expressed in the different packing schemes of these basic *AnQ* polyhedra. Many of these structures have no counterparts in lanthanide or transition-metal chemistry. Because of the diffuse nature of the 5*f* orbitals, as well as the tendency of the chalcogenides for catenation and covalent bond formation, the concept of formal oxidation state is of limited utility and its assignment is often not possible. Nor can one correlate the results of magnetic susceptibility measurements with structures. Clearly, new syntheses, detailed structural studies, and concomitant magnetic susceptibility and conductivity measurements are needed to bring order and predictability to this area of solid-state chemistry.

Acknowledgment. This work was supported by NSF Grant No. DMR97-09351. J.A.I. acknowledges the great loss he feels with the death of Jean Rouxel—gentleman, superb scientist, and friend.

References

(1) Zachariasen, W. H. *Acta Crystallogr.* **1948**, *1*, 265−268.
(2) D'Eye, R. W. M.; Sellman, P. G.; Murray, J. R. *J. Chem. Soc.* **1952**, 2555−2562.
(3) D'Eye, R. W. M. *J. Chem. Soc.* **1953**, 1670−1672.
(4) D'Eye, R. W. M.; Sellman, P. G. *J. Chem. Soc.* **1954**, 3760−3766.
(5) Zumbusch, M. *Z. Anorg. Allg. Chem.* **1940**, *243*, 322−329.
(6) Snyder, R. L.; Nichols, M. C.; Boehme, D. R. *Powder Diffract.* **1991**, *6*, 204−227.
(7) Graham, J.; McTaggart, F. K. *Aust. J. Chem.* **1960**, *13*, 67−73.
(8) Daoudi, A.; Levet, J. C.; Potel, M.; Noël, H. *Mater. Res. Bull.* **1996**, *31*, 1213−1218.
(9) Noël, H.; Padiou, J.; Prigent, J. *C. R. Séances Acad. Sci., Ser. C* **1971**, *272*, 206−208.
(10) Noël, H. *C. R. Séances Acad. Sci., Ser. C* **1973**, *277*, 463−464.
(11) Julien, R.; Rodier, N.; Tien, V. *Acta Crystallogr., Sect. B: Struct. Crystallogr. Cryst. Chem.* **1978**, *34*, 2612−2614.
(12) Noël, H. *C. R. Séances Acad. Sci., Ser. C* **1974**, *279*, 513−515.
(13) Noël, H.; Padiou, J.; Prigent, J. *C. R. Séances Acad. Sci., Ser. C* **1975**, *280*, 123−126.
(14) Chenevier, B.; Wolfers, P.; Bacmann, M.; Noël, H. *C. R. Acad. Sci., Sér. 2* **1981**, *293*, 649−652.
(15) Noël, H.; Padiou, J. *Acta Crystallogr., Sect. B: Struct. Crystallogr. Cryst. Chem.* **1976**, *32*, 1593−1595.
(16) Daoudi, A.; Noël, H. *J. Less-Common Met.* **1989**, *153*, 293−298.
(17) Daoudi, A.; Noël, H. *Inorg. Chim. Acta* **1987**, *140*, 93−95.
(18) Brochu, R.; Padiou, J.; Grandjean, D. *C. R. Séances Acad. Sci., Ser. C* **1970**, *271*, 642−643.
(19) Lelieveld, R.; IJdo, D. J. W. *Acta Crystallogr., Sect. B: Struct. Crystallogr. Cryst. Chem.* **1980**, *36*, 2223−2226.
(20) Noël, H. *Rev. Chim. Miner.* **1977**, *14*, 295−299.
(21) We ignore structural results based solely on X-ray powder data; for example, we choose not to discuss a number of quaternary mixed-3d metal compounds of the type $MM'U_2Q_6$ that have been characterized by this technique.[22,23]
(22) Slovyanskikh, V. K.; Kuznetsov, N. T.; Kvaratskheliya, T. A. *Russ. J. Inorg. Chem.* (*Engl. Transl.*) **1991**, *36*, 25.
(23) Slovyanskikh, V. K.; Kuznetsov, N. T. *Russ. J. Inorg. Chem.* **1992**, *37*, 1365.
(24) Slovyanskikh, V. K.; Kuznetsov, N. T.; Gracheva, N. V. *Russ. J. Inorg. Chem.* (*Engl. Transl.*) **1984**, *29*, 960−961.
(25) Noël, H.; Prigent, J. *Physica B+C* (*Amsterdam*) **1980**, *102*, 372−379.
(26) Tien, V.; Guittard, M.; Flahaut, J.; Rodier, N. *Mater. Res. Bull.* **1975**, *10*, 547−554.
(27) Brochu, R.; Padiou, J.; Prigent, J. *C. R. Séances Acad. Sci., Ser. C* **1972**, *274*, 959−961.
(28) Brochu, R.; Padiou, J.; Prigent, J. *C. R. Acad. Sci. Paris* **1970**, *270*, 809−810.
(29) Potel, M.; Brochu, R.; Padiou, J. *Mater. Res. Bull.* **1975**, *10*, 205−208.
(30) Noël, H.; Potel, M.; Padiou, J. *Acta Crystallogr., Sect. B: Struct. Crystallogr. Cryst. Chem.* **1976**, *32*, 605−606.

(31) Narducci, A. A.; Ibers, J. A. *Inorg. Chem.* **1998**, *37*, 3798−3801.
(32) Potel, M.; Brochu, R.; Padiou, J.; Grandjean, D. *C. R. Séances Acad. Sci., Ser. C* **1972**, *275*, 1419−1421.
(33) Noël, H.; Potel, M.; Padiou, J. *Acta Crystallogr., Sect. B: Struct. Crystallogr. Cryst. Chem.* **1975**, *31*, 2634−2637.
(34) Kohlmann, H.; Stöwe, K.; Beck, H. P. *Z. Anorg. Allg. Chem.* **1997**, *623*, 897−900.
(35) Tien, V.; Rodier, N. *C. R. Séances Acad. Sci., Ser. C* **1979**, *289*, 17−20.
(36) Stocks, K.; Eulenberger, G.; Hahn, H. *Z. Anorg. Allg. Chem.* **1981**, *472*, 139−148.
(37) Haneveld, A. J. K.; Jellinek, F. *J. Less-Common Met.* **1969**, *18*, 123−129.
(38) Pietraszko, D.; Lukaszewicz, K. *Bull. Acad. Pol. Sci., Ser. Sci. Chim.* **1975**, *23*, 337−340.
(39) Zygmunt, A.; Murasik, A.; Ligenza, S.; Leciejewicz, J. *Phys. Status Solidi A* **1974**, *22*, 75−79.
(40) Beck, H. P.; Dausch, W. *Z. Anorg. Allg. Chem.* **1989**, *571*, 162−164.
(41) Trzebiatowski, W.; Niemiec, J.; Sepichowska, A. *Bull. Acad. Pol. Sci., Ser. Sci. Chim.* **1961**, *9*, 373−377.
(42) Haneveld, A. J. K.; Jellinek, F. *J. Inorg. Nucl. Chem.* **1964**, *26*, 1127−1128.
(43) Mansuetto, M. F.; Jobic, S.; Ng, H. P.; Ibers, J. A. *Acta Crystallogr., Sect. C: Cryst. Struct. Commun.* **1993**, *49*, 1584−1585.
(44) Zachariasen, W. H. *Acta Crystallogr.* **1949**, *2*, 291−296.
(45) Hulliger, F. *J. Less-Common Met.* **1968**, *16*, 113−117.
(46) Kaczorowski, D.; Noël, H.; Potel, M.; Zygmunt, A. *J. Phys. Chem. Solids* **1994**, *55*, 1363−1367.
(47) Amoretti, G.; Blaise, A.; Burlet, P.; Gordon, J. E.; Troc, R. *J. Less-Common Met.* **1986**, *121*, 233−248.
(48) Benz, R.; Zachariasen, W. H. *Acta Crystallogr., Sect. B: Struct. Crystallogr. Cryst. Chem.* **1969**, *25*, 294−296.
(49) Benz, R.; Zachariasen, W. H. *Acta Crystallogr., Sect. B: Struct. Crystallogr. Cryst. Chem.* **1970**, *26*, 823−827.
(50) Breeze, E. W.; Brett, N. H. *J. Nucl. Mater.* **1971**, *40*, 113−115.
(51) Noël, H.; Potel, M.; Shlyk, L.; Kaczorowski, D.; Troc, R. *J. Alloys Compd.* **1995**, *217*, 94−96.
(52) Guittard, M.; Vovan, T.; Julien-Pouzol, M.; Jaulmes, S.; Laruelle, P.; Flahaut, J. *Z. Anorg. Allg. Chem.* **1986**, *540/541*, 59−66.
(53) Jaulmes, S.; Julien-Pouzol, M.; Dugué, J.; Laurelle, P.; Vovan, T.; Guittard, M. *Acta Crystallogr., Sect. C: Cryst. Struct. Commun.* **1990**, *46*, 1205−1207.
(54) Simon, A.; Peters, K.; Peters, E.-M. *Z. Anorg. Allg. Chem.* **1982**, *491*, 295−300.
(55) Do, J. W.; Kim, J. W.; Lah, S. M.; Yun, H. S. *Bull. Korean Chem. Soc.* **1993**, *14*, 678−681.
(56) Daoudi, A.; Potel, M.; Noël, H. *J. Alloys Compd.* **1996**, *232*, 180−185.
(57) Chevrel, R.; Sergent, M.; Prigent, J. *J. Solid State Chem.* **1971**, *3*, 515−519.
(58) Daoudi, A.; Lamire, M.; Levet, J. C.; Noël, H. *J. Solid State Chem.* **1996**, *123*, 331−336.
(59) Noël, H.; Potel, M. *J. Less-Common Met.* **1985**, *113*, 11−15.
(60) Noël, H. *J. Less-Common Met.* **1980**, *72*, 45−49.
(61) Daoudi, A.; Noël, H. *Inorg. Chim. Acta* **1986**, *117*, 183−185.
(62) Daoudi, A.; Noël, H. *J. Less-Common Met.* **1986**, *115*, 253−259.
(63) Daoudi, A.; Noël, H. *J. Solid State Chem.* **1985**, *60*, 131−134.
(64) Rodier, N.; Tien, V. *Acta Crystallogr., Sect. B: Struct. Crystallogr. Cryst. Chem.* **1976**, *32*, 2705−2707.
(65) Daoudi, A.; Noël, H. *J. Alloys Compd.* **1996**, *233*, 169−173.
(66) Sunshine, S. A.; Kang, D.; Ibers, J. A. *J. Am. Chem. Soc.* **1987**, *109*, 6202−6204.
(67) Cody, J. A.; Mansuetto, M. F.; Pell, M. A.; Chien, S.; Ibers, J. A. *J. Alloys Compd.* **1995**, *219*, 59−62.
(68) Tougait, O.; Daoudi, A.; Potel, M.; Noël, H. *Mater. Res. Bull.* **1997**, *32*, 1239−1245.
(69) Wu, E. J.; Pell, M. A.; Ibers, J. A. *J. Alloys Compd.* **1997**, *255*, 106−109.
(70) Cody, J. A.; Ibers, J. A. *Inorg. Chem.* **1996**, *35*, 3836−3838.
(71) Beck, H. P.; Dausch, W. *Z. Naturforsch., B: Chem. Sci.* **1988**, *43*, 1547−1550.
(72) Furuseth, S.; Brattås, L.; Kjekshus, A. *Acta Chem. Scand. Ser. A* **1975**, *29*, 623−631.
(73) Furuseth, S.; Fjellvåg, H. *Acta Chem. Scand.* **1991**, *45*, 694−697.
(74) Cody, J. A.; Ibers, J. A. *Inorg. Chem.* **1995**, *34*, 3165−3172.
(75) Slovyanskikh, V. K.; Kuznetsov, N. T. *Russ. J. Inorg. Chem.* (*Engl. Transl.*) **1990**, *35*, 447.
(76) Slovyanskikh, V. K.; Kuznetsov, N. T.; Gracheva, N. V. *Russ. J. Inorg. Chem.* (*Engl. Transl.*) **1985**, *30*, 314−315.
(77) Slovyanskikh, V. K.; Kuznetsov, N. T.; Gracheva, N. V. *Russ. J. Inorg. Chem.* (*Engl. Transl.*) **1989**, *34*, 1388.
(78) Kuznetsov, N. T.; Slovyanskikh, V. K.; Gracheva, N. V. *Russ. J. Inorg. Chem.* (*Engl. Transl.*) **1979**, *24*, 1749−1750.
(79) Wu, P.; Christuk, A. E.; Ibers, J. A. *J. Solid State Chem.* **1994**, *110*, 337−344.
(80) Christuk, A. E.; Wu, P.; Ibers, J. A. *J. Solid State Chem.* **1994**, *110*, 330−336.
(81) Wu, P.; Ibers, J. A. *J. Solid State Chem.* **1994**, *110*, 156−161.
(82) Pell, M. A.; Ibers, J. A. *J. Alloys Compd.* **1996**, *240*, 37−41.
(83) Sutorik, A. C.; Albritton-Thomas, J.; Hogan, T.; Kannewurf, C. R.; Kanatzidis, M. G. *Chem. Mater.* **1996**, *8*, 751−761.
(84) Narducci, A. A.; Ibers J. A., unpublished results.
(85) Padiou, J.; Guillevic, J. *C. R. Séances Acad. Sci., Ser. C* **1969**, *268*, 822−824.
(86) Cody, J. A.; Ibers, J. A. *Inorg. Chem.* **1994**, *33*, 2713−2715.
(87) Chondroudis, K.; Kanatzidis, M. G. *C. R. Acad. Sci. Paris* **1996**, *322*, 887−894.
(88) Chondroudis, K.; Kanatzidis, M. G. *J. Am. Chem. Soc.* **1997**, *119*, 2574−2575.
(89) Gillespie, R. J. *Chem. Soc. Rev.* **1992**, *21*, 59−69.
(90) Burdett, J. K.; Hoffmann, R.; Fay, R. C. *Inorg. Chem.* **1978**, *17*, 2553−2568.
(91) Pell, M. A.; Ibers, J. A. *Chem. Ber.* **1997**, *130*, 1−8.
(92) Shannon, R. D. *Acta Crystallogr., Sect. A: Cryst. Phys., Diffr., Theor. Gen. Crystallogr.* **1976**, *32*, 751−767.
(93) Noël, H. *J. Solid State Chem.* **1984**, *52*, 203-210.

CM9802200